Laser and Particle Beams (2003), *21*, 403–409. Printed in the USA.

DOI: 10.1017/S0263034603213185

Mix experiments using a two-dimensional convergent shock-tube

D.A. HOLDER, A.V. SMITH, C.J. BARTON, AND D.L. YOUNGS
Atomic Weapons Establishment, Reading, Berkshire, United Kingdom

(RECEIVED 12 April 2002; ACCEPTED 4 April 2003)

Abstract

This article reports the first Richtmyer–Meshkov instability experiments using an improved version of the Atomic Weapons Establishment convergent shock tube. These investigate the shock-induced turbulent mixing across the interfaces of an air/dense gas/air region. Multipoint ignition of a detonatable gas mixture produces a cylindrically convergent shock that travels into a test cell containing the dense gas region. The mixing process is imaged with shadowgraphy. Sample results are presented from an unperturbed experiment and one with a notch perturbation imposed on one of the dense gas interfaces. The unperturbed experiment shows the mixing across the dense gas boundaries and the motion of the bulk dense gas region. Imposition of the notch perturbation produces a mushroom-shaped air void penetrating the dense gas region. Three-dimensional simulations performed using the AWE TURMOIL3D code are presented and compared with the sample experimental results. A very good agreement is demonstrated. Conducting these first turbulent mixing experiments has highlighted a number of areas for future development of the convergent shock-tube facility; these are also presented.

Keywords: Compressible turbulent mixing; Convergent shock tube; Laser sheet technique; Richtmyer–Meshkov instability

1. INTRODUCTION

At the 7th International Workshop on the Physics of Compressible Turbulent Mixing (IWPCTM) preliminary experiments were reported (Holder *et al.*, 1999) that provided an early indication of the likely feasibility of the oxy-acetylene driven atomic weapons establishment (AWE) convergent shock tube (CST) for Richtmyer–Meshkov (RM) instability mix experiments. Several improvements have since been introduced leading to a demonstration of RM mixing experiments in convergent geometry using air and SF_6 gas both with and without a perturbation imposed on one of the gas boundaries. The improvements have resulted from an exhaustive investigation into identifying and understanding those design and operating elements crucial to achieving satisfactory cylindrical shock formation and convergence. The existing CST prototype is awaiting replacement by a new CST design featuring laser sheet visualization in place of the current shadowgraphy technique. While awaiting this successor CST, the results presented are to be regarded as preliminary, with the shortcomings of applying shadowgraphy imaging to turbulent gas mixing clearly evident.

The presented images showing the mixing process during the compression and expansion phases are seen to provide satisfying comparison with calculations performed using the TURMOIL3D code.

Address correspondence and reprint requests to: D.A. Holder, Bldg. H27, AWE, Aldermaston, Reading, Berkshire, RG7 4PR, Great Britain. E-mail: david.holder@awe.co.uk

2. CONVERGENT SHOCK TUBE DESIGN

Figure 1 shows the shock tube consisting of four gas zones partitioned within a wedge-shape structure of 30° apex angle and outer radius 1.025 m. Spacing between the two slab sides is 50 mm. The lower zone (60 mm radial depth) contains approximately 2 L of oxy-acetylene gas mixture acting as the driver gas, sealed by thin aluminum foil at the top, ignited by 30 spark plugs at the periphery. The zones above contain, respectively, air, dense gas (sulphur hexafluoride), and air, all at atmospheric pressure, with separation achieved by the use of microfilm membranes supported on fine wire meshes as developed in the related AWE 200 × 100 mm shock-tube experiments. The upper region is manufactured from a 25-mm clear acrylic sheet of demountable construction to enable insertion of the membrane and wire mesh

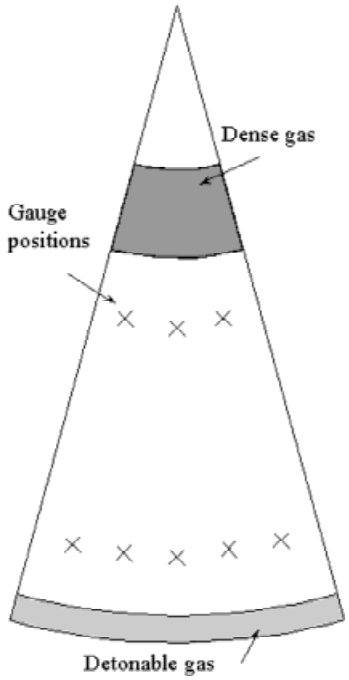

Fig. 1. Illustration of CST design.

assemblies. The 50-mm-wide side sections of the dense gas zone feature small bore flow channels designed to ensure complete displacement of the contained air by the dense gas during the purging and filling process while offering only a minimal leak path during the shock compression process. Flow into the apex is terminated at radius 30 mm due to the insertion of a solid wedge. It was originally fitted to avoid possible mechanical damage to the apex and consequent leakage of high pressure gases: latterly it has been regarded as suitably physically representative of a proposed lens assembly designed to form a divergent laser sheet to illuminate and interrogate the mixing process. Its presence is included in all code calculations.

3. DETAILS OF EXPERIMENTS PERFORMED

Two mix experiments are described, referred to as a "basic" experiment and the "notch" experiment, as in Figure 2. They differ only by the inclusion of a notch, dimensioned as shown, on the lower air/SF_6 gas boundary.

Figure 2 shows details of the gas confinement. Both microfilm membranes are sandwiched between wire meshes or parallel (z-direction) wire arrays. Meshes above the membranes provide a fragmentation action on upward shock acceleration of the membranes: wire arrays beneath minimize distortion of the membrane under the hydrostatic pressure of the dense gas. The wire meshes, of 50 μm diameter tungsten, feature a 4 mm $\times$ 4 mm aperture; the wire arrays use an 8-mm spacing.

Small-bore passageways within the side walls of the assemblies provide vent paths to aid the purge process and ensure complete filling of the gas chambers. Their effect on the shock passage is negligible due to the small dimensions of the holes and the relatively high shock and flow velocities.

4. SHOCK PRESSURE WAVEFORMS

Figure 1 indicates the location of the pressure transducers installed within the nonoptical section of the CST: three at radius 0.5 m, five at radius 0.8 m. Recording the shock arrival times reveals any departure from completely cylindrical progression of the shock front. Further, from the arrival times at the two radii, the mean shock velocity could be determined, so providing a measure of the performance of the oxy-acetylene driver. The sample pressure versus time signature in Figure 3, recorded at radius 0.5 m, identifies the shocks propagating within the system. The only significant distinction between each group of pressure waveforms is evident in arrival time variations of ± 1 μs, equivalent to a ± 1-mm departure from the mean cylindrical radius.

The detonation process produces an equivalent quasi-static pressure of about 15–20 bar, dependent on oxy-acetylene gas composition. It drives an air shock of

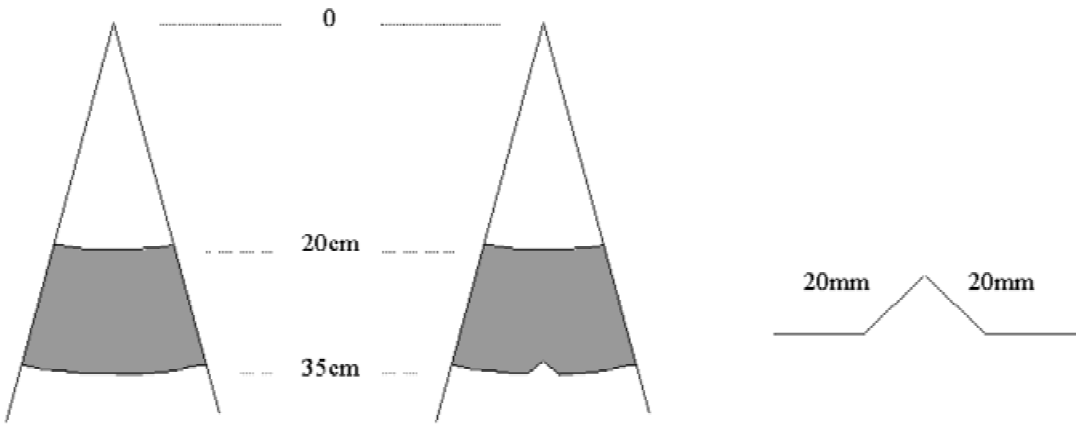

Fig. 2. Schematic of experimental configuration.

https://doi.org/10.1017/S0263034603213185 Published online by Cambridge University Press

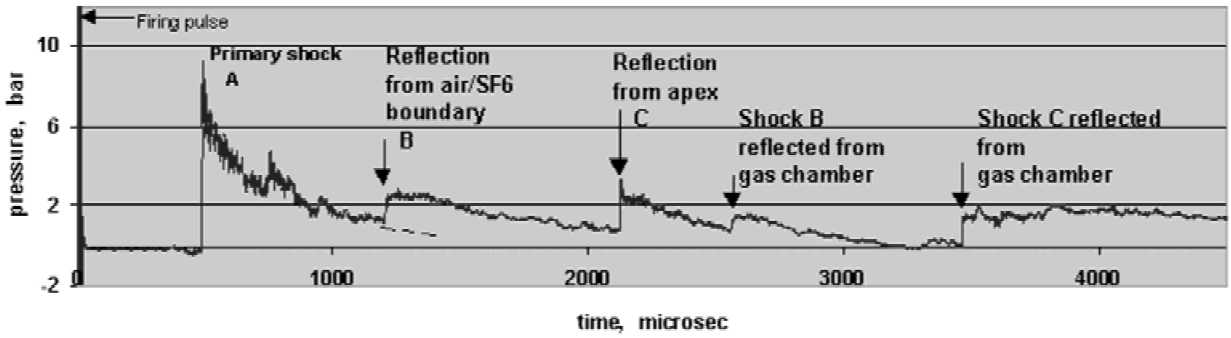

Fig. 3. Pressure waveform recorded at radius 0.50 m.

approximately 10 bar peak pressure into the air beyond the aluminum foil. The shock and foil velocities are, respectively, 1095 and 825 m/s. The pressure subsequently slightly reduces but tends to recover before the shock reaches the dense gas interface.

5. DETONATION SYSTEM

The main features of the detonatable gas chamber are its ignition system, the gas diffusers, and the method of supporting the diaphragm. The ignition system comprises 30 miniature spark plugs (i.e., at 1° intervals) fed by parallel cables (with current monitors) from a 10-kV, 25-J capacitor discharge unit. The spark plugs are flush mounted in the base of the gas chamber. The thin aluminum foil diaphragm is clamped between the upper and lower halves of the gas chamber; its profile is maintained by contact with an array of wires that prevent foil distortion during the gas pressurization process. Filling and purging of the gas chamber takes place through porous inserts to aid diffusion of the oxy-acetylene gas and a homogeneous gas fill. Their relatively high flow impedance minimizes losses of the high-pressure detonated gas products through the inlet and gas outlet ports

The volume of the gas chamber is approximately 2 L, with a fill time of several minutes. At completion of the purging process, the detonatable gas supply is stopped and the gas chamber allowed to relax to atmospheric pressure before sealing.

To check for simultaneity of multipoint detonation, a small optical test cell representing a 1/10 volume of the gas chamber was constructed. This features three spark plugs and allows photographic study of the detonation process. A photograph of this small detonation test cell is shown in Figure 4 alongside shadowgraphs from a single experiment. These show (bottom) the three detonation waves, one from each spark plug, fusing together in the oxy-acetylene mixture and (top) the aluminum foil diaphragm with the air shock ahead of it. This illustrates that the spacing of the three spark plugs is sufficiently small to produce a virtually plane shock. A series of experiments conducted on this small test cell provided further evidence to support these observations and also demonstrated the reliability of the current system.

6. MIX EXPERIMENT RESULTS

Following a successful series of experiments using the small detonation test cell, the detonation system was considered to have demonstrated sufficient reliability to justify conducting Richtmyer–Meshkov turbulent mixing experiments using the CST. The first tests were "basic" mix experiments with plane (i.e., unperturbed; Fig. 2) interfaces. Sample results from one of these experiments are shown in Figure 5.

The success of the plane interface basic experiments led to undertaking a perturbed experiment with a triangular notch perturbation (Fig. 2) imposed on the lower interface. Only one experiment was fired in this configuration; sample results are shown in Figure 6. Unfortunately, water trapped in the multiple thickness membrane used for the lower interface smeared along the window of the test cell during shock passage, obscuring some of the image. This will be eliminated in further experiments. However, the major feature, a mushroom-shaped air cavity can still be observed propagating into the dense gas region. At 1.20 ms after shock arrival at the lower interface, two jets of dense gas are seen travelling up the angled walls of the test cell ahead of

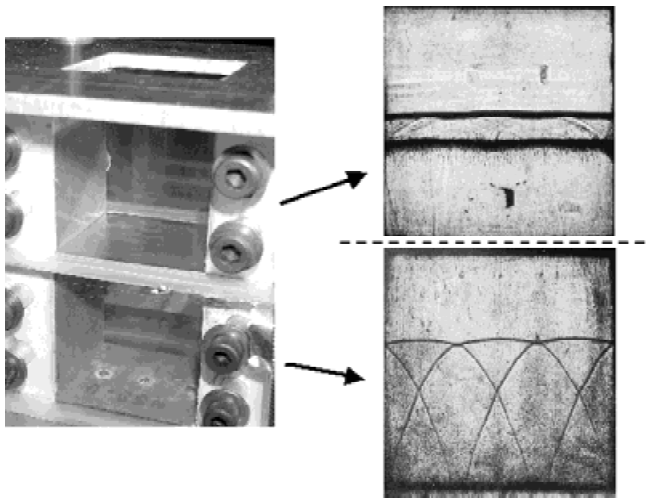

Fig. 4. Small detonation test cell and two images from one experiment showing detonation waves (bottom) and resulting air shock (top).

https://doi.org/10.1017/S0263034603213185 Published online by Cambridge University Press

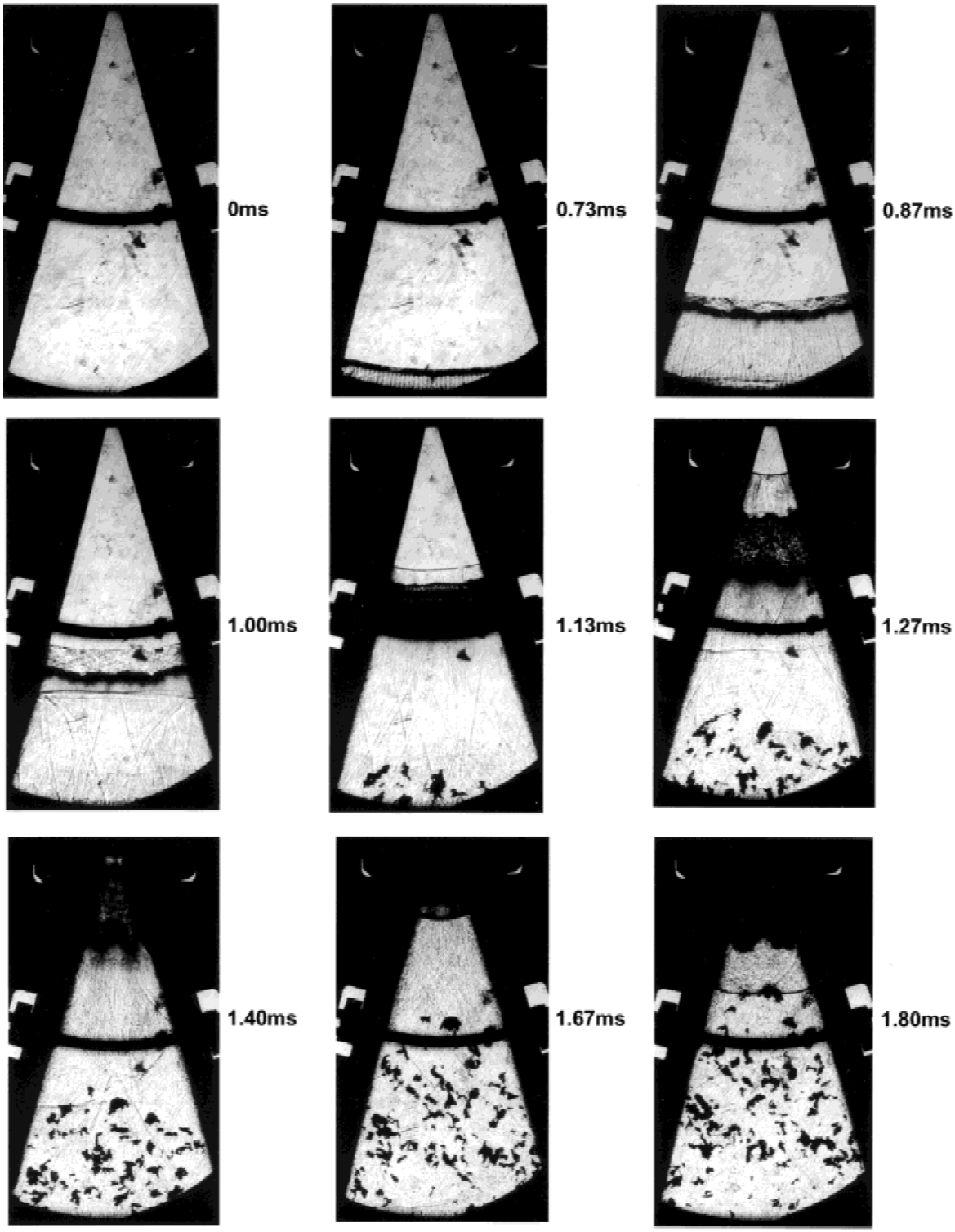

Fig. 5. Sample results from one plane experiment.

the bulk dense gas region; this is in close agreement with the code predictions in the next section. An assessment of the effect of boundary layers in the results is also discussed in Section 8.

7. CODE SIMULATION

As for the linear shock tube experiments (Holder *et al.*, 2003) the AWE TURMOIL 3D code has been used to model

https://doi.org/10.1017/S0263034603213185 Published online by Cambridge University Press

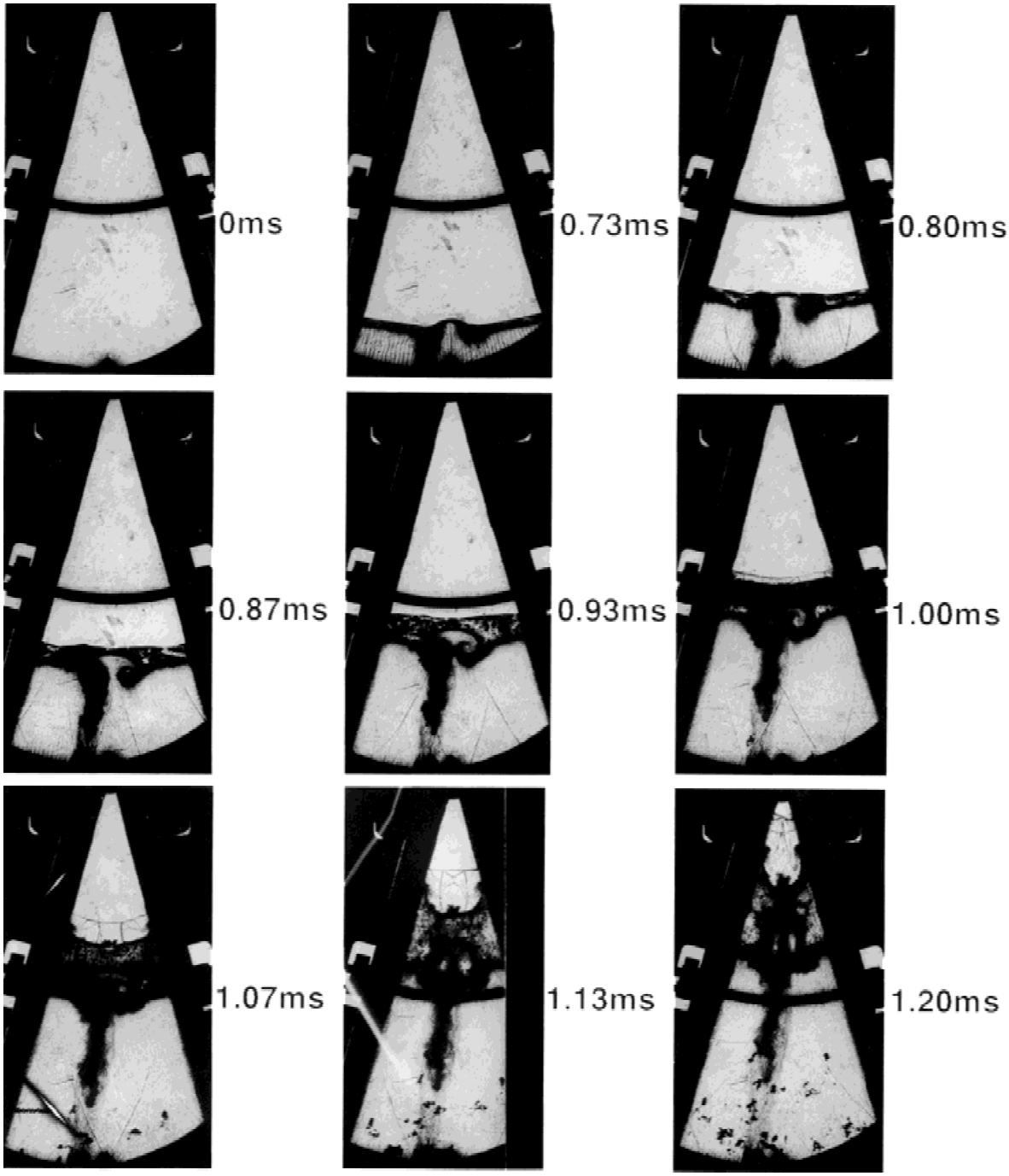

Fig. 6. Sample results from one notch experiment.

the CST experiments. In this case, a cylindrical polar mesh is used. A semi-Lagrangian calculation is performed where radial zoning moves with the mean fluid velocity, illustrated in Figure 7. Zoning in the three-dimensional (3D) region (r, θ, z) is $344 \times 200 \times 140$.

Perfect gas equations of state are used ($\gamma = 1.060$ for SF_6, $\gamma = 1.401$ for air). Initial perturbations were applied to the inner and outer air/SF_6 interfaces to represent the effect of membrane rupture. The random amplitude (ζ) perturbations were of the form

$$\zeta(\theta, z) = S \sum_{m,n\geq 0} \cos 6m\theta \left(a_{mn} \cos \frac{2n\pi z}{L} + b_{mn} \sin \frac{2n\pi z}{L} \right).$$

https://doi.org/10.1017/S0263034603213185 Published online by Cambridge University Press

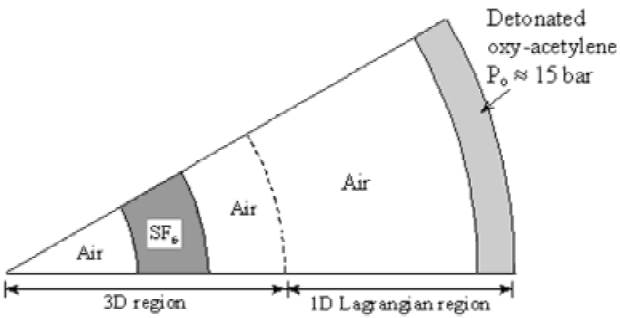

Fig. 7. Illustration of code regions.

The wavelength, λ, for mode (m,n) is given by

$$\frac{1}{\lambda^2} = \frac{1}{\lambda_\theta^2} + \frac{1}{\lambda_z^2}$$

where

$$\lambda_\theta = \frac{\pi R}{3m}, \qquad \lambda_z = \frac{L}{n},$$

R is the radius of the interface, and L is the width of the shock tube. Modes are included for which $0.5\text{ cm} < \lambda < 5\text{ cm}$ and in that case, the coefficients are chosen from a Gaussian distribution with unit s.d. Finally the scaling factor S is chosen to give $\sqrt{\langle \zeta^2 \rangle} = 0.01$ cm.

A comparison of experimental images with their corresponding code images is shown in Figure 8. Slight time differences exist between code output times and experimental image capture times. However, strong similarities are clearly evident.

8. DISCUSSION

Qualitative comparison between the experimental and code images shows very good agreement. Due to the high level of agreement, this comparison can be used to infer the significance of boundary layer effects. The 3D simulation uses free slip boundaries, that is, there is no viscous interaction of the gases with the walls. This, therefore, suggests that there is little significance of boundary layer effects in the experimental results. However, some further work should be carried out to confirm this.

To enable future quantitative comparison between experimental images and simulations, a laser sheet diagnostic will be required, as used in other experiments by the authors (Smith *et al.*, 1999). A fluorescent seeding agent will be employed such that the light intensity recorded by the cam-

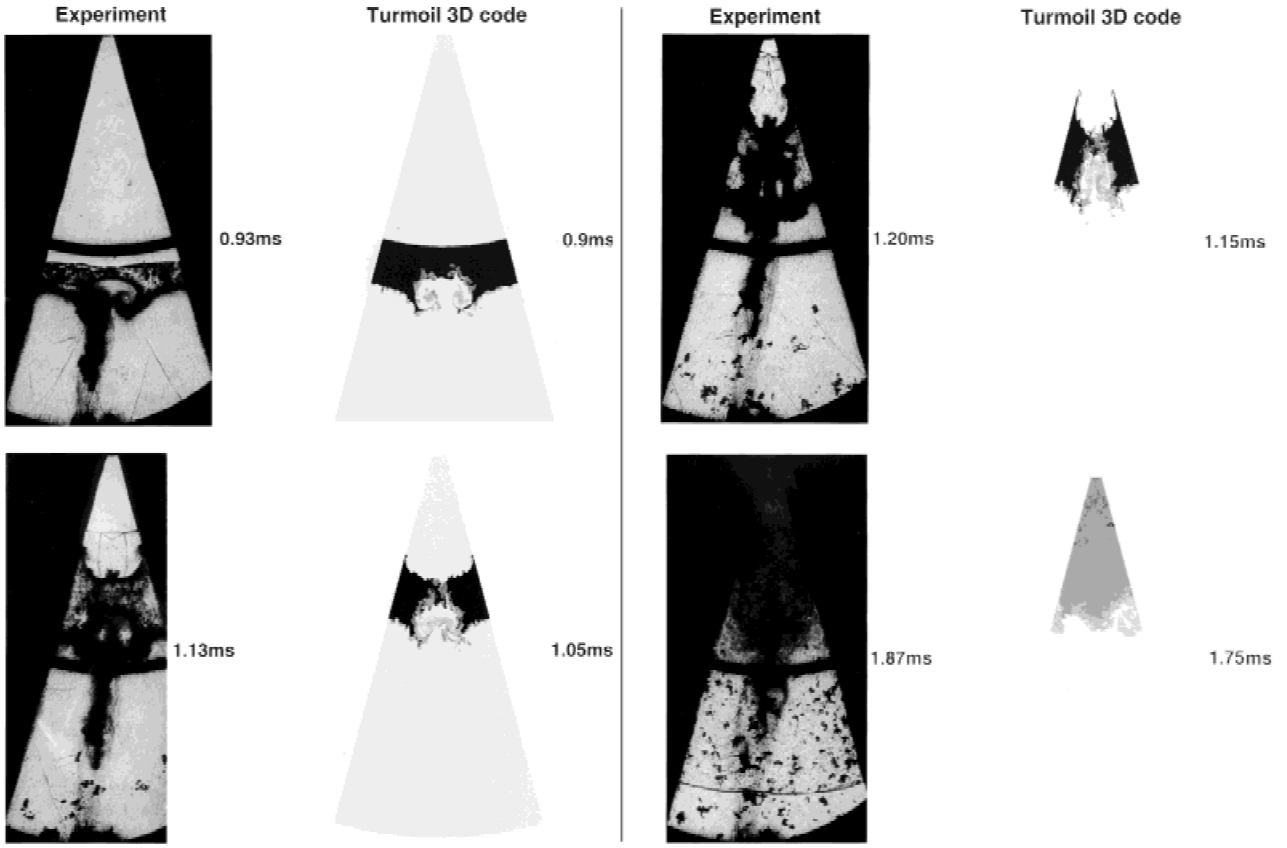

Fig. 8. Comparison of sample experimental and code images.

https://doi.org/10.1017/S0263034603213185 Published online by Cambridge University Press

era will be directly proportional to the seeding concentration and hence the dense gas concentration. Therefore, the intensity images would, after calibration, be compared directly with the concentration information of the simulations. In this manner, a quantity could be defined that would provide a measure of the comparison.

9. CONCLUSIONS

AWE has successfully demonstrated the suitability of a convergent shock tube for performing Richtmyer–Meshkov mixing experiments with gases in 2D convergent geometry.

The CST has achieved compressions of dense gas estimated at 25:1 using a shock Mach number of approximately 3. Results from an unperturbed experiment and one with a notch perturbation imposed on one dense gas boundary have been presented. Comparison between the experimental results and those from simulations has shown very good agreement. This agreement appears to indicate no significant boundary layer effects. However, a laser sheet diagnostic and analysis of future experiments will be required to obtain a quantitative comparison.

These mix experiments together with those on the small optical detonation cell have ensured the achievement of good understanding of the design requirements for constructing a new improved CST. A number of areas for improvement have been identified and are presented in the following section.

10. FUTURE WORK

Construction of a new convergent shock tube that operates with the laser sheet diagnostic and any future variations is planned as a priority. In addition to improvements identified by this current work, it is anticipated that seeding with fluorescent gas or particles will be established in the new design. This will enable use of a notch filter to filter out incident wavelength reflections while allowing recording of the fluorescent signal. The new seeding must be suitable for seeding at high gas compressions.

It is proposed that further experiments be performed with different perturbation profiles on the current facility while construction of a new facility is underway. Substituting xenon gas for sulphur hexafluoride will enable the TURMOIL3D code to use an equation of state that is more clearly defined, which should improve agreement with the experimental data. Additionally, calibration techniques will be established for gas data analysis of laser sheet images for quantitative comparison between experimental and code data.

Investigation of wall effects should be undertaken by splitting the notch perturbation and locating each half at an angled wall boundary (equivalent to shifting the experiment 15° around a full 360° version of the CST with notches at 30° intervals).

REFERENCES

Holder, D.A., Smith, A.V., Philpott, M.K. & Millar, D.B. (1999). First mix experiments on the AWE convergent shock tube. *Proc. 7th Int. Workshop on the Physics of Compressible Turbulent Mixing*. (Meshkov, E., Yanilkin, Yu. & Zhmailo, V., Eds.). pp. 28–32. Sarov, Russia: RFNC-VNITEF.

Holder, D.A., Smith, A.V. & Youngs, D.L. (2003). Shock tube experiments on Richtmyer–Meshkov instability growth using an enlarged double bump perturbation. *Laser Part. Beams* **21**, 411–418.

Smith, A.V., Holder, D.A., Philpott, M.K. & Millar, D.B. (1999). Notch and double bump experiments using the 200 × 100 mm linear shock tube. *Proc. 7th Int. Workshop on the Physics of Compressible Turbulent Mixing*. (Meshkov, E., Yanilkin, Yu. & Zhmailo, V., Eds.). pp. 124–130. Sarov, Russia: RFNC-VNITEF.

https://doi.org/10.1017/S0263034603213185 Published online by Cambridge University Press